



Probiotics *Lactobacillus reuteri* Abrogates Immune Checkpoint Blockade-Associated Colitis by Inhibiting Group 3 Innate Lymphoid Cells

Tingting Wang¹, Naisheng Zheng¹, Qin Luo¹, Li Jiang², Baokun He^{3,4}, Xiangliang Yuan^{1*} and Lisong Shen^{1*}

¹ Department of Clinical Laboratory, Xinhua Hospital, Shanghai Jiao Tong University School of Medicine, Shanghai, China, ² Department of Gynecology and Obstetrics, Xinhua Hospital, Shanghai Jiao Tong University School of Medicine, Shanghai, China, ³ Department of Gastroenterology, Shanghai General Hospital, Shanghai Jiao Tong University School of Medicine, Shanghai, China, ⁴ Shanghai Key Laboratory of Pancreatic Disease, Shanghai General Hospital, Shanghai Jiao Tong University School of Medicine, Shanghai, China

OPEN ACCESS

Edited by:

Anna Kathleen Coussens,
University of Cape Town, South Africa

Reviewed by:

Marina Sandra Palermo,
National Council for Scientific and
Technical Research
(CONICET), Argentina
Maryam Dadar,
Razi Vaccine and Serum Research
Institute, Iran

*Correspondence:

Xiangliang Yuan
yuanxiangliang@gmail.com
Lisong Shen
lisongshen@hotmail.com

Specialty section:

This article was submitted to
Microbial Immunology,
a section of the journal
Frontiers in Immunology

Received: 04 March 2019

Accepted: 15 May 2019

Published: 04 June 2019

Citation:

Wang T, Zheng N, Luo Q, Jiang L,
He B, Yuan X and Shen L (2019)
Probiotics *Lactobacillus reuteri*
Abrogates Immune Checkpoint
Blockade-Associated Colitis by
Inhibiting Group 3 Innate Lymphoid
Cells. *Front. Immunol.* 10:1235.
doi: 10.3389/fimmu.2019.01235

Immune checkpoint blockade (ICB) immunotherapy increases antitumor immunity by blocking cytotoxic-T-lymphocyte-associated protein 4 (CTLA-4) or programmed cell death protein 1 (PD-1)/programmed death-ligand 1 (PD-L1) and displays robust clinical responses in various cancers. However, ICB immunotherapy also triggers severe inflammatory side effects, known as immune-related adverse effects (irAEs). One of the most common toxicities is immune checkpoint blockade-associated colitis (ICB associated colitis). The exact mechanism of ICB associated colitis remains to be explored. Here, we combined ICB (anti-CTLA-4 and anti-PD-1) treatment with a standard colitis model, in which a more severe form of colitis is induced in mice, to recapitulate the clinical observations in patients receiving combined ipilimumab (anti-CTLA-4) and nivolumab (anti-PD-1) therapy, during which colitis is the most frequent complication encountered. We found that the composition of the gut microbiota changed in ICB associated colitis. Principal component analysis of the gut microbiome showed an obvious reduction in the abundance of *Lactobacillus* in severe ICB associated colitis. *Lactobacillus* depletion completely by vancomycin augmented the immunopathology of ICB. Furthermore, we found that the ICB toxicity could be totally eliminated via the administration of a widely available probiotic *Lactobacillus reuteri* (*L. reuteri*). Oral administration of *L. reuteri* therapeutically inhibited the development and progression of colitis, thus ameliorating the loss of body weight and inflammatory status induced by ICB treatment. Mechanistically, the protective effect of *L. reuteri* was associated with a decrease in the distribution of group 3 innate lymphocytes (ILC3s) induced by ICB associated colitis. In conclusion, our study highlights the immunomodulatory mechanism of the gut microbiota and suggests that manipulating the gut microbiota by administering *L. reuteri* can mitigate the autoimmunity induced by ICB, thus allowing ICB immunotherapy to stimulate the desired immune response without an apparent immunopathology.

Keywords: immune checkpoint blockade, colitis, gut microbiome, inflammation, innate lymphoid cells

INTRODUCTION

Immune checkpoint blockade (ICB) immunotherapy targeting intrinsic downregulators of immunity, such as cytotoxic T-lymphocyte-associated antigen 4 (CTLA-4), programmed cell death protein 1 (PD-1), and programmed cell death ligand 1 (PD-L1) has shown durable clinical responses and recently been a source of promising new cancer treatments (1, 2). ICB Immunotherapy has transformed the oncology field, improving survival in patients suffering from a range of cancer types. To date, several immune-checkpoint-blocking mAbs have been approved for the treatment of patients with several types of cancer, and more and more patients will benefit from ICB immunotherapy in the months and years ahead.

While ICB immunotherapy stimulates T-cell activation and effective antitumor immune responses, it can also have serious inflammatory side effects in some patients, known as immune-related adverse effects (irAEs), which resemble autoimmune disease (3). irAEs are frequent and might occur in up to 90% of patients treated with the anti-CTLA-4 antibody (4) and in 70% of patients treated with a PD-1/PD-L1 antibody (5). Although any organ system can be affected, irAEs most commonly involve the gastrointestinal tract, endocrine glands, skin, and liver (6). One of the most common toxicities is immune checkpoint blockade-associated colitis (ICB associated colitis) (7). ICB associated colitis can be quite severe and represents a distinct form of colitis with characteristics reminiscent of inflammatory bowel disease (IBD) (8, 9). Clinically, ICB-associated colitis is routinely treated with immunosuppressive therapy, which diminishes the antitumor response of ICB and has significant side effects (10). Recommendations regarding the optimal management of ICB associated colitis need to be evolved (10, 11). Recently, several reports from cohorts of ICB-treated patients suffering from colitis have confirmed the similarities between ICB-associated colitis and IBD both clinically and endoscopically (8). There is significant overlap between the conditions, including the development of deep ulceration, a negative prognostic factor. Histologically, ICB-associated colitis exhibits features of chronic damage, including IBD- and lymphocytic colitis-like phenotypes. The immunopathogenesis of ICB-associated colitis appears to be predominantly associated with mucosal Th1/Th17 effector responses (12). However, the exact mechanism underlying ICB-associated colitis remains to be identified. Uncovering the mechanisms involved in its pathogenesis will greatly enhance our understanding and therapeutic management of ICB-mediated colitis.

Recently, several studies have started to highlight the crucial role of the gut microbiota in the antitumor responses induced by checkpoint blockade antibodies (6, 7). The composition of the gut microbiota has been shown to affect antitumor immune responses (13–17). A rapidly expanding concept is that the gut

microbiome affects not only the efficacy of the treatment but also the toxicity due to ICB. Indeed, novel evidence supports the idea that in both anti-CTLA-4 and anti-PD-1 colitis, specific “favorable” or “unfavorable” microbiome profiles may affect the efficacy of the immune response and, consequently, the appearance of gastrointestinal irAEs (18, 19). The syndromes of irAEs mostly frequently affect the gastrointestinal tract and the skin which exposed to commensal microorganisms. However, a knowledge gap remains regarding how the gut microbiota influences gastrointestinal irAEs. *L. reuteri* are Gram-positive, rod-shaped, and anaerobic. As a common bacterial strain coexisting in human and animal gastrointestinal tract, *L. reuteri* has been confirmed that have many excellent probiotic characteristics. First, LR secretes antibacterial substances such as lactic acid, hydrogen peroxide to regulate intestinal pH and microenvironment to inhibit the colonization of pathogenic microbes and remodel the commensal microbiota (20). A recent study indicated that *L. reuteri* can also induce anti-inflammatory Treg cells, and mediate suppression of Th1/Th2 responses (21). Also, bearing the ability to strengthen the intestinal barrier, the colonization of *L. reuteri* may decrease the inflammation in the gut. It has been confirmed by several studies that *L. reuteri* can alleviate DSS induced colitis by inhibiting proinflammatory gene expression (22) and reducing P-selectin-associated leukocyte- and platelet-endothelial cell interactions (23). However, the effect of *L. reuteri* on the appearance of gastrointestinal irAEs is underexplored.

In the present study, we established a dextran sulfate sodium (DSS)-induced colitis and B16 melanoma tumor mouse model to imitate the clinical outcomes of patients receiving ipilimumab (Anti-CTLA-4) and nivolumab (anti-PD-1), for whom colitis is the most frequent problem encountered. We conducted this model to study the impact of the composition of the gut microbiota on the immunopathology of ICB-associated colitis, and explore the therapeutic way to mitigate ICB-induced autoimmunity by manipulating the gut microbiota to allow checkpoint blockade to achieve the desired immune response.

MATERIALS AND METHODS

Mouse Strains

C57BL/6 mice were purchased from SLAC Laboratory Animals Co., Ltd. (Shanghai, China). For all of the experiments, 8 weeks old female mice were used. The mice were maintained in the Shanghai Laboratory Animal Center of China. The mouse experiments were approved by the Ethics Committee of Xinhua Hospital, Shanghai Jiao Tong University School of Medicine.

Cell Lines

The B16 cell line was purchased from Shanghai Institutes for Biological Sciences (Shanghai, China), and the cells were cultured in RPMI Medium 1640 (Gibco, Life Technologies, USA) containing 10% FBS (Gibco, USA), 100 U/mL penicillin, and 100 µg/mL streptomycin, at 37°C in a humidified atmosphere of 5% CO₂.

Abbreviations: ICB, Immune Checkpoint Blockade; CTLA-4, cytotoxic-T-lymphocyte-associated protein 4; PD-1, programmed cell death protein 1 (PD-1); PD-L1, programmed death-ligand 1; irAEs, immune-related adverse effects; DSS, dextran sulfate sodium; *L. reuteri*, *Lactobacillus reuteri*; ILC, innate lymphocytes.

Generation of Inflammation Mouse Models

The mice received 3% DSS (MP Biomedicals) in their drinking water for 10–15 d. Weight was recorded daily. For the gut commensal manipulation, mice were treated with vancomycin (0.5 g/L, Sigma, USA) in the drinking water for at least 14 d. Afterward, DSS was added to their drinking water. For ICB-associated colitis, The mice were injected once every other day (initiated 3 day before the DSS administration) with 100 μ g of anti-CTLA-4 mAb (Bioxcell, USA) and 250 μ g of anti-PD-1 mAb (Bioxcell, USA) or isotype control antibody before the DSS administration.

Tumor Challenges and Animal Treatment

2×10^5 B16 tumor cells were subcutaneously (s.c.) injected into the right flanks of the mice. The mice were injected intraperitoneally (i.p.) with 100 μ g of anti-CTLA-4 mAb and 250 μ g of anti-PD-1 four times after 7, 10, 13, and 16 days of tumor incubation. Tumor size was measured with a caliper and calculated as the length \times width \times width \times 0.5236.

L. reuteri Administration

L. reuteri ATCC PTA 6475 cells resuspended in PBS were used in this study. Each mouse was given 300 μ L of *L. reuteri* (1×10^9 CFU per mouse) via oral gavage. In the DSS colitis and tumor model, *L. reuteri* was administered daily before the DSS administration or tumor injection for 3 days until the samples collected.

Tissue Isolation and Flow Cytometry Assay

For tumor isolation, B16 tumor explants were removed after euthanizing the mice. The isolated tumors were cut into small pieces with scissors. Next, the pieces were digested with collagenase Type IV (1 mg/mL; Worthington, USA), DNase I (0.02 mg/mL; Sigma-Aldrich, USA), hyaluronidase (0.1 mg/mL; BBI Life Sciences, USA) at 37°C for 30 min. The tumor samples were then pressed through 70 μ m nylon filters (BD Biosciences, USA) to create single-cell suspensions. For the colon isolation: The colon was carefully dislodged, while simultaneously removing the mesenteric fat. The caecum was removed, and the colons were placed into cold PBS to remove most of the feces. The samples were incubated in Hank's balanced salt solution with 5 mM EDTA (Invitrogen, USA) and without calcium or magnesium (Beyotime, China) at 37°C with agitation (120 rpm) three times for 20 min each time. Scissors were used to cut the gut into small pieces, and the pieces were digested in Hank's balanced salt solution with calcium and magnesium (Beyotime, China) supplemented with collagenase Type IV (1 mg/mL; Worthington, USA), DNase I (500 μ g/mL; Sigma-Aldrich, USA), dispase (200 μ g/mL; Sigma, USA), and 2% FCS at 37°C for 20 min. The samples were then pressed through 70 μ m nylon filters (BD Biosciences, USA). The digestion was repeated three times, and 40 and 80% Percoll solutions were used (Yeasten, China) to disrupt the cells to create single-cell suspensions. For the FACS analysis, the cells were stained with antibodies to the following markers: CD45 (clone 30-F11), CD3 (clone 17A2), CD3 (clone 145-2C11), CD4 (clone GK1.5), CD8a (clone 53-6.7), GR-1 (clone 1A8), CD19 (clone 1D3), CD127

(IL7Ra) (clone A7R34), ROR γ t (clone Q31-378), NKp46 (clone 29A1.4), KLRG-1 (clone 2F1/KLRG1), CD11b (clone M1/70), Ly-6G (clone RB6-8C5), ki67 (clone SolA15). All of the antibodies were produced by BD, eBioscience, or Biolegend and are listed in **Supplementary Table S1**. Dead cells were excluded from the analysis using Fixable Viability Dye eFluor 450 (eBioscience, USA). For the intranuclear staining, the cells were fixed and permeabilized using the Foxp3 staining kit (eBioscience, USA). All of the flow experiments were performed on FACS Canto II machines (BD, USA), and the flow cytometry data were analyzed with FlowJo 10.

Colitis Scores and Histologic Analysis

Freshly isolated colons were fixed in formalin and embedded in paraffin. H&E staining was performed using a standard protocol. For the quantitative histological analysis, five criteria were used to grade each section of the intestine: (i) severity of inflammation, (ii) percent of area affected by inflammation, (iii) degree of hyperplasia, (iv) depth of the lesion, and (v) ulceration.

16S rRNA Gene Sequencing and Analyses

The genomic DNA contained in the stool samples was extracted using an extraction kit (E.Z.N.ATM Mag-Bind Soil DNA Kit, Omega, USA) according to the manufacturer's instructions. We measured the concentration of the DNA using a Qubit 2.0 (life, USA) to ensure that adequate amounts of high-quality genomic DNA had been extracted and the DNA quality assessed using a bioanalyzer (Agilent 2100, USA). The PCR was performed immediately after the DNA was extracted. The V3-V4 region of the bacterial 16S rRNA gene was amplified using the universal primers (24, 25) 341F (CCTACGGGNGGCWGCAG) and 805R (GACTACHVGGGTATCTAATCC). The reaction was set up as follows: microbial DNA (10 ng/ μ L) 2 μ L; amplicon PCR forward primer (10 μ M) 1 μ L; amplicon PCR reverse primer (10 μ M) 1 μ L; 2 \times KAPA HiFi Hot Start Ready Mix 15 μ L (total 30 μ L). The plate was sealed and PCR performed in a thermal instrument (Applied Biosystems 9700, USA) using the following program: 1 cycle of denaturing at 95°C for 3 min, first 5 cycles of denaturing at 95°C for 30 s, annealing at 45°C for 30 s, elongation at 72°C for 30 s, then 20 cycles of denaturing at 95°C for 30 s, annealing at 55°C for 30 s, elongation at 72°C for 30 s and a final extension at 72°C for 5 min. The PCR products were checked using electrophoresis in 1% (w/v) agarose gels in TBE buffer (Tris, boric acid, EDTA) stained with ethidium bromide (EB) and visualized under UV light. The PCR products were checked using electrophoresis in 1% (w/v) agarose gels in TBE buffer (Tris, boric acid, EDTA) stained with ethidium bromide (EB) and visualized under UV light. We used AMPure XP beads to purify the free primers and primer dimer species in the amplicon product. Barcodes unique to each sample were incorporated at the beginning of the forward primers, which allowed the identification of each sample in a mixture during an Illumina sequencing run. The sequencing was performed using the Illumina MiSeq system (Illumina MiSeq, USA) according to the manufacturer's instructions. The rarefaction curves and the diversity indices were determined based on the calculated

operational taxonomic units (OTUs) by Mothur ver. 1.30.1. The obtained sequences were phylogenetically sorted to the phylum, class and genus levels at 97% similarity for the community composition analysis. For the taxonomic analysis, the representative sequences from each OTU were subjected to the RDP-II Classifier of the Ribosomal Database Project (RDP) and the BLAST algorithm of the National Center for Biotechnology Information (NCBI). The 16S rRNA sequence data have been deposited in the NCBI BioProject with accession number PRJNA525923.

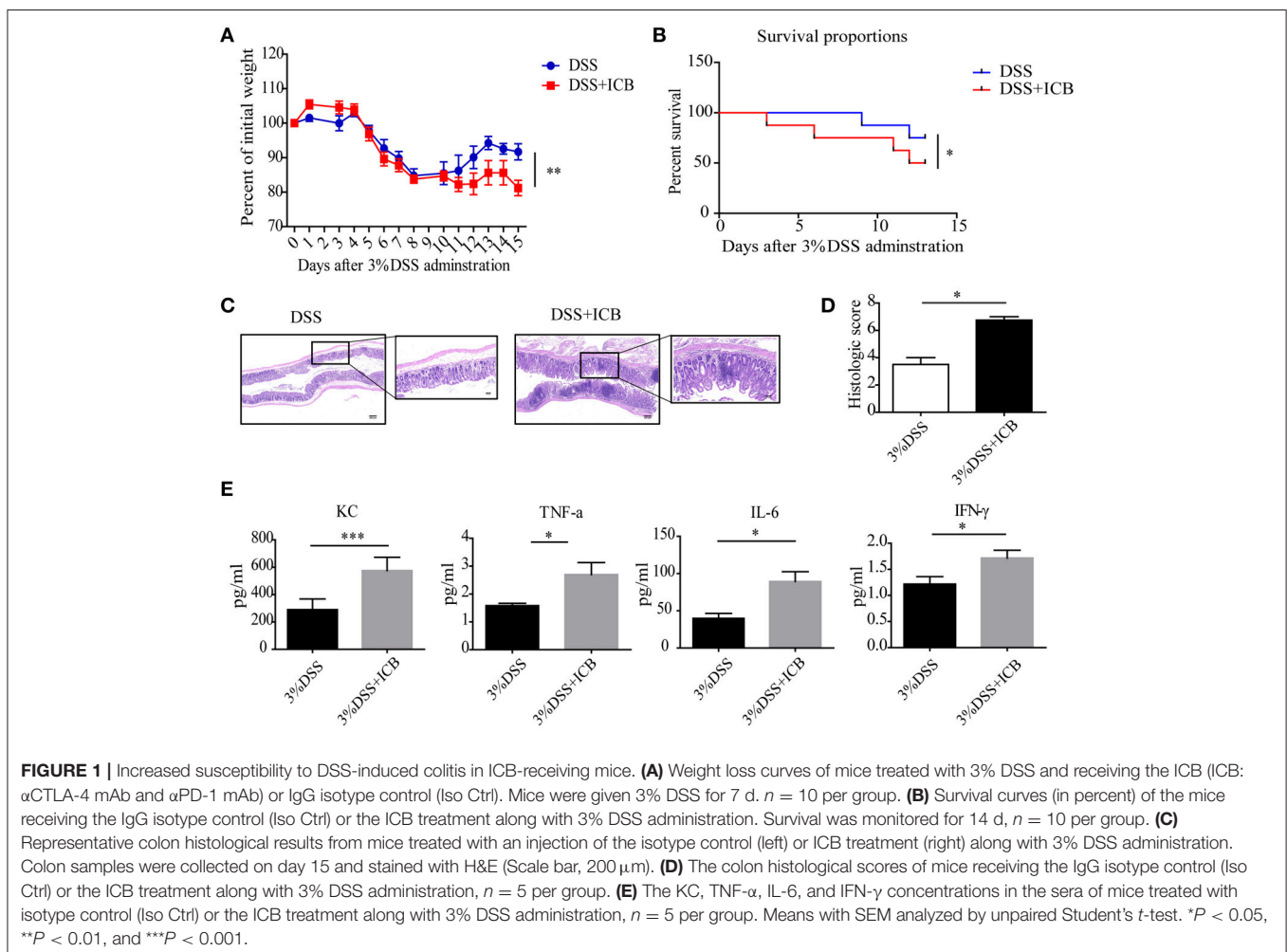
Serum Cytokine Analysis

Blood samples were collected on one time point on day 10 (DSS + ICB + Van group) or day 15 (DSS group/ICB+DSS group/*L.reuteri* group) days according to the weight loss of mice after colitis induction with DSS. After clotting for at least 30 min at room temperature, the plasma was separated in a centrifuge (10 min at 1,500 relative centrifugal force). The secreted plasma levels of a range of inflammatory cytokines (CXCL1, TNF- α , IL-12 p70, IL-1 β , IL-2, IL-4, IL-6, IL-10, IL-13, IFN- γ) were assessed using a mouse Magnetic Luminex Assay Kit (R&D Systems, USA) and quantified using a Luminex multiplexing suspension array system (LUMINEX X-200, R&D, USA) following the

manufacturer's instructions. The cytokines of IL-23, IL-22, and IL-17 in intestine tissues and sera of mice were assessed using the mouse ELISA Assay Kits (R&D Systems, USA) following the manufacturer's instructions.

Statistical Analysis

In each experiment, multiple mice were analyzed as biological replicates. All of the statistical analyses were performed using GraphPad Prism 7.0 software and displayed as the mean \pm SEM. The statistical significance of any differences was assessed using Student's *t*-test, and one-way ANOVA was conducted for multiple comparisons. For the survival analysis, Kaplan-Meier survival curves were calculated, and the statistical significance was determined by the log-rank test. In the analysis of the component differences between groups, Welch's *t*-test and one-way ANOVA with the Tukey-Kramer *post-hoc* test were used via STAMP. The eta-squared (η^2) value was used to estimate the effect size. Differences were considered statistically significant when the *p*-value was <0.05 , and the significance levels are represented by **P* < 0.05 , ***P* < 0.01 , ****P* < 0.001 , and *****P* < 0.0001 , unless denoted otherwise. The 16S rRNA sequence data have been deposited in the NCBI BioProject with accession number PRJNA525923.



RESULTS

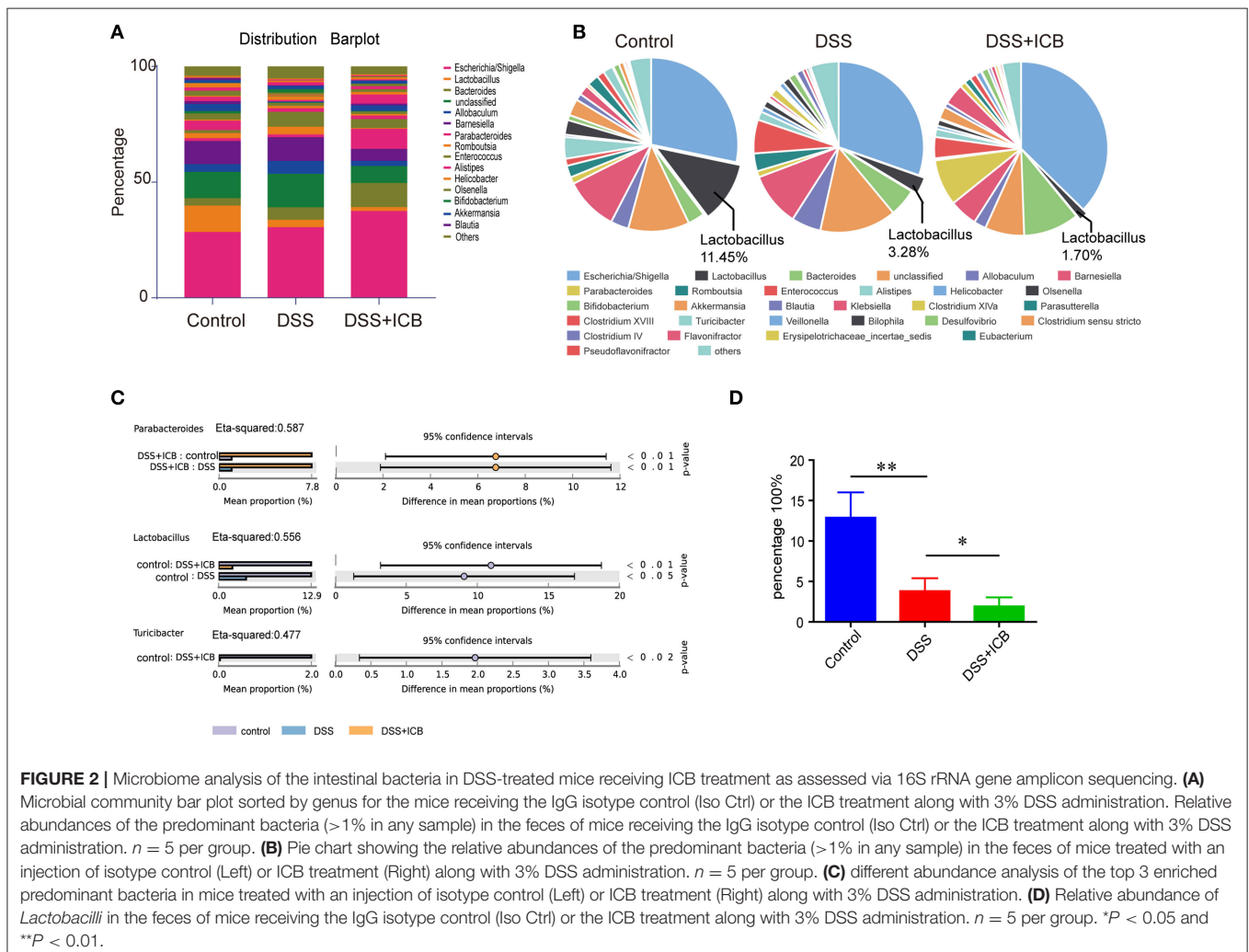
ICB Treatment Increased the Susceptibility of DSS-Induced Colitis in ICB Receiving Mice

Clinically, immune checkpoint blockade (ICB)-associated colitis closely resembles the colitis associated with IBD pathophysiology (8). To establish a checkpoint blockade-related autoimmune mouse model, mice were tested to determine their response to orally administered dextran sulfate sodium (DSS) with an injection of a combination of anti-CTLA-4 and anti-PD-1 antibodies or isotype control. After administration of 3% DSS via the drinking water for 7 days, the mice that received ICB treatment showed more severe weight loss compared to that of mice that received the isotype control antibody (Figures 1A,B). There was significantly efficacy without significant weight loss in ICB treated mice in the absence of DSS (Supplementary Figures S1, S2). Histological colonic sections from the ICB associated mice model (Supplementary Figure S3A) showed that the animals that received the ICB combined treatment

exhibited more severe exacerbated hyperplasia, more inflammatory leukocyte infiltration, and severe ulceration compared with the mice that received DSS without ICB treatment but isotype control antibody, resulting in poorer histopathological scores (Figures 1C,D). The serum levels of four inflammatory cytokines, KC, TNF- α , IL-6, and IFN- γ were dramatically increased in the ICB-treated mice (Figure 1E, Supplementary Figure S3B). Furthermore, we observed a therapeutic effect of the combination treatment with anti-CTLA-4 and anti-PD-1 antibody against established B16 melanomas in the same mice (Supplementary Figures S1A–C), as reported previously. Thus, the data from our B16 tumor model and DSS-induced colitis are consistent with clinical observations in patients who received ipilimumab (anti-CTLA-4 antibody), and/or nivolumab (anti-PD-1 antibody), for whom colitis is the most commonly encountered problem.

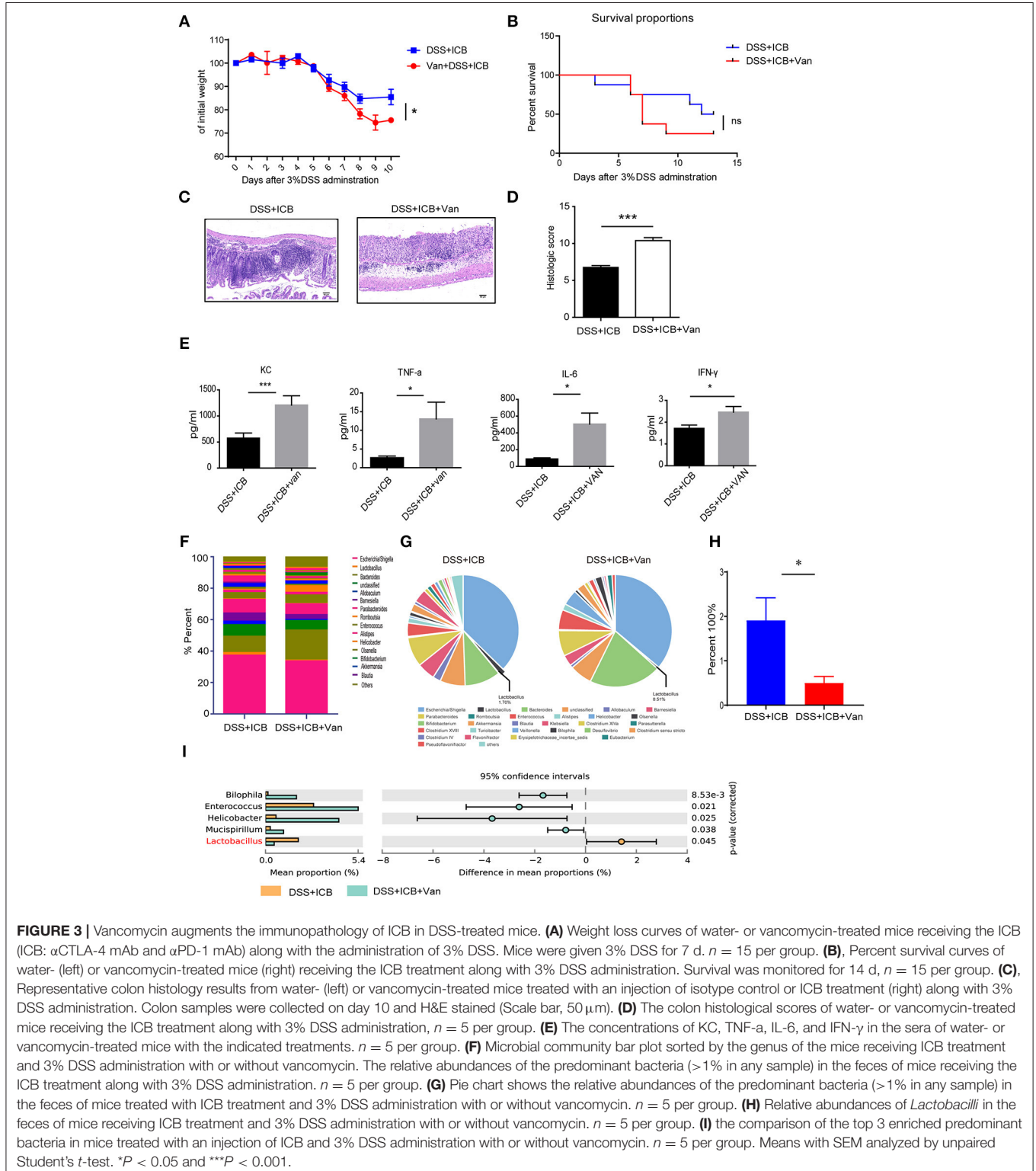
The Immunopathology of ICB Associated Colitis Impacts the Gut Microbiota

Several lines of evidence support a critical role for the microbiota in the experimental colitis system (26). To determine the changes



in the commensal bacteria composition with the development of ICB related colitis, fecal samples collected from mice receiving the IgG isotype control (Iso Ctrl) or the ICB treatment along with 3% DSS administration were submitted for bacterial microbiota

profiling using 16S ribosomal RNA sequencing on the Illumina MiSeq platform. The histograms in **Figure 2A** illustrate the gut microbiota community structures and reveal the microbial species and their relative abundances. As shown in **Figure 2B**, all



of the samples contained *Escherichia*, *Lactobacillus*, *Bacteroides*, *Allobaculum*, *Barnesiella*, and *Parabacteroides*. Analysis of the results showed that the relative abundances of *Parabacteroides*, *Lactobacillus*, and *Turicibacter* were significantly different among the three groups (Figure 2C). The most abundant phyla were *Escherichia*, *Allobaculum*, and *Lactobacillus*, and the least abundant phylum was *Lactobacillus* in the mice that received ICB treatment with 3% DSS administration (Figures 2C,D). Hierarchical clustering of the samples based on the relative abundance of the bacterial species also revealed that the relative population of *Lactobacillus* was significantly lower in the stool of ICB-treated mice compared to that in the stool from mice in the control and DSS administration only groups ($P < 0.01$; Figure 2D).

Depletion of *Lactobacillus* by Vancomycin Augments the Immunopathology of ICB

Lactobacillus is a genus of Gram-positive anaerobic bacteria. We wondered if depletion of *Lactobacillus* by vancomycin (an antibiotic activity against Gram-positive bacteria, including lactobacillus) would impact the severity of ICB-associated colitis. Previously, a study showed that vancomycin exacerbates histopathological signs of gut inflammation (16). To test whether the loss of *Lactobacillus* or other strains contributed to the severe colitis, we assessed the impact of vancomycin on the colitis severity after ICB treatment in the DSS colitis model. The mice were pretreated with vancomycin for 2 weeks before

the induction of colitis. In the vancomycin group, the mice started to show lower body weight from 6 d of DSS with ICB treatment (Figure 3A), showing more severe colitis that occurs in the absence of antibiotic treatment. Consistently, more severe weight loss was observed in mice pretreated with vancomycin than in mice that received the water control (Figure 3A). By day 9, 80% of the vancomycin plus DSS and ICB-treated mice had died, whereas only 20% of mice given the water control had died (Figure 3B). The histopathological scores were also significantly worse for the vancomycin-treated mice than for the controls (Figure 3C). H&E staining of colon sections showed complete ulceration and severe immune cell infiltration in the vancomycin-treated mice (Figure 3D). Similar serum levels of three inflammatory cytokines, KC, TNF- α , IL-6, and IFN- γ , were also dramatically increased in the vancomycin-treated mice (Figure 3E and Supplementary Figure S4). Furthermore, stool microbiome analyses also confirmed that vancomycin administration decreased the *Lactobacillus* abundance to an undetectable level (Figures 3F-I).

Direct Administration of *L. reuteri* Ameliorates the Immunopathology of ICB

To directly test the protective effect of the probiotic *Lactobacillus* in this colitis model, we obtained a commercially available probiotic *L. reuteri* and administered the bacteria to the mice via oral gavage before the induction of DSS colitis (Supplementary Figure S5A). This probiotic *L. reuteri*

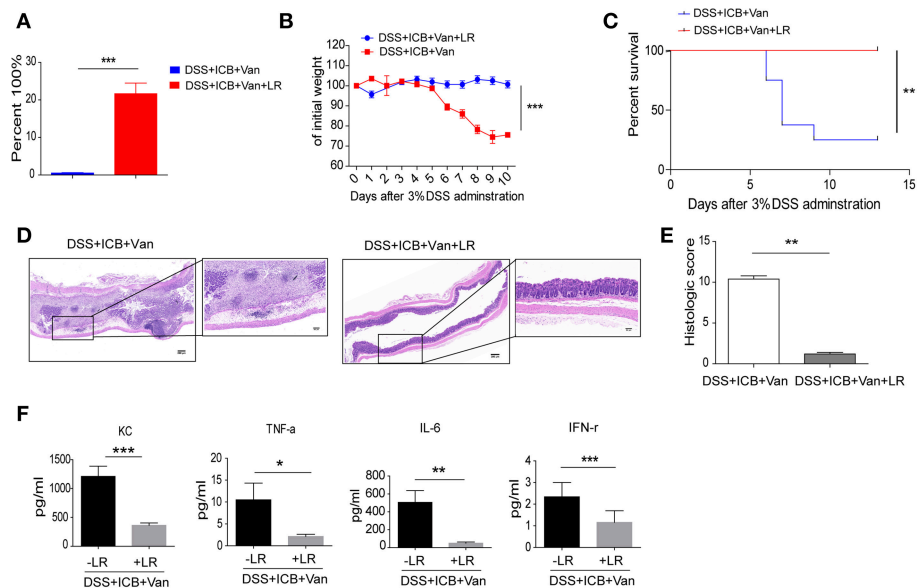
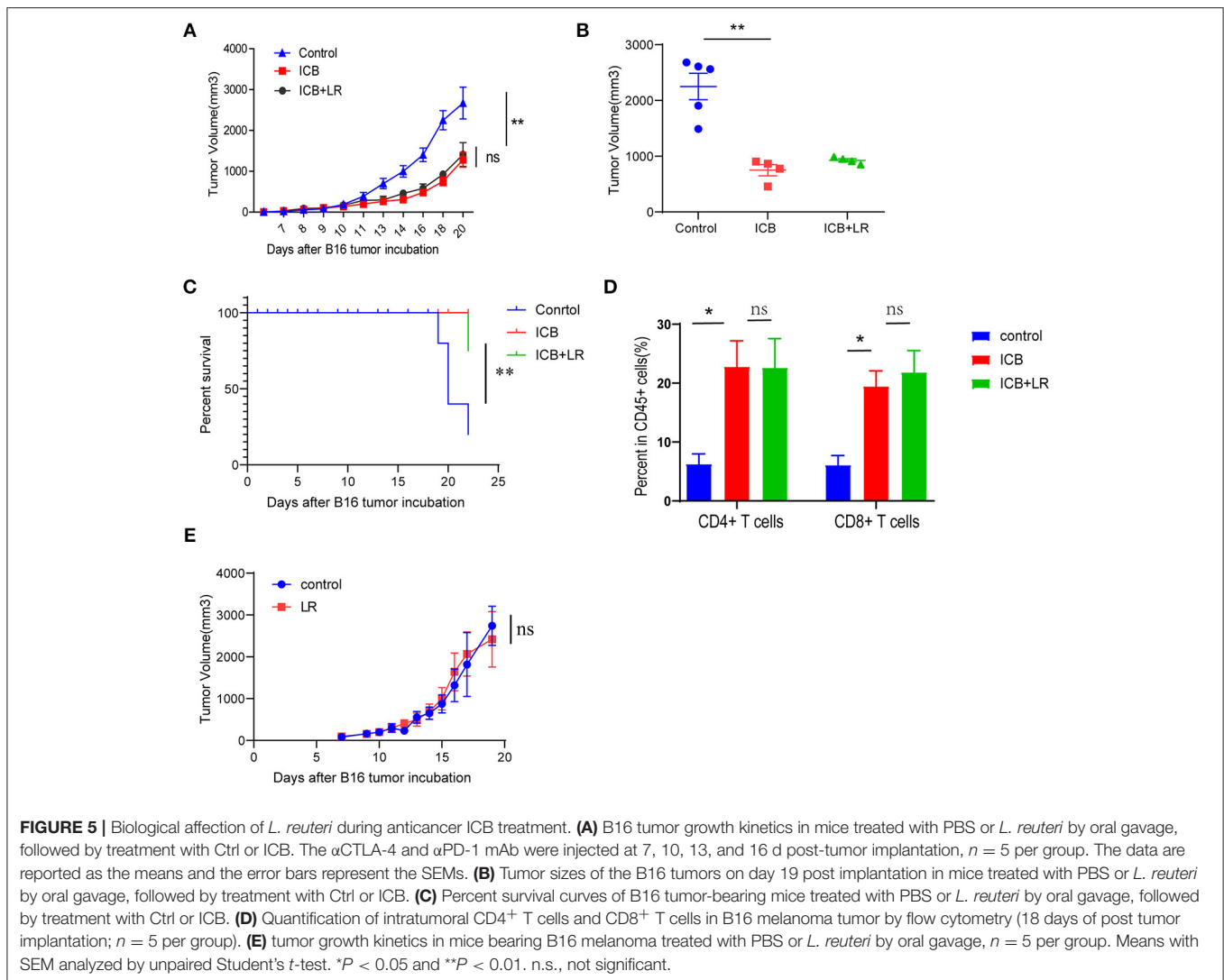


FIGURE 4 | *L. reuteri* therapeutically abrogates ICB-associated intestinal inflammation in DSS-treated mice. **(A)** The relative abundance of *L. reuteri* was quantified with 16s RNA sequencing. This value was normalized to the total bacteria, $n = 5$ per group. $***P < 0.001$. **(B)** Weight loss curves of ICB-injected mice with 3% DSS-induced colitis treated either with vancomycin + PBS, or vancomycin + *L. reuteri*, $n = 15$ per group. **(C)** Percent survival curves of in ICB-injected mice with 3% DSS-induced colitis treated as described in A. Survival was monitored for 14 d, $n = 15$ per group. **(D)** Representative colonic histology results from ICB-injected mice with 3% DSS-induced colitis with the indicated treatments. Colon samples were collected on day 10 and H&E stained (Scale bar, 200 μ m) **(E)** Quantification of the colon histological scores of ICB-injected mice with 3% DSS-induced colitis treated as described in A, $n = 5$ per group. **(F)** Serum concentrations of KC, TNF- α , IL-6, and IFN- γ in the serum of ICB-injected mice with 3% DSS-induced colitis with the indicated treatments, $n = 5$ per group. Means with SEM analyzed by unpaired Student's *t*-test. $*P < 0.05$, $**P < 0.01$, and $***P < 0.001$.



treatment resulted in a 20-fold increase in the relative abundance of these bacteria in the feces (Figure 4A and Supplementary Figures S5B–D). Under our combined ICB conditions, *L. reuteri* treatment improved ICB induced colitis (Supplementary Figures S6A–E). *L. reuteri* administration completely rescued the severe weight loss induced by vancomycin and ICB treatment in the DSS colitis model mice (Figures 4B,C). The average weight of the vancomycin-treated mice was improved from 70% of their initial weight in the DSS plus ICB group to almost 100% in the *L. reuteri* group on day 10 after DSS administration (Figure 4B). Mice treated with both *L. reuteri* and vancomycin exhibited no weight loss (Figure 4B), suggesting that *L. reuteri* treatment ameliorated the immunopathology associated with ICB by helping to rescue the vancomycin-induced gut dysbiosis. Consistent with this assessment, H&E staining of colon sections also revealed that *L. reuteri* treatment resulted in a reduced histopathological score with partial restoration of the colon structure and less leukocyte infiltration in gut tissue (Figures 4D,E). Similarly, *L. reuteri*

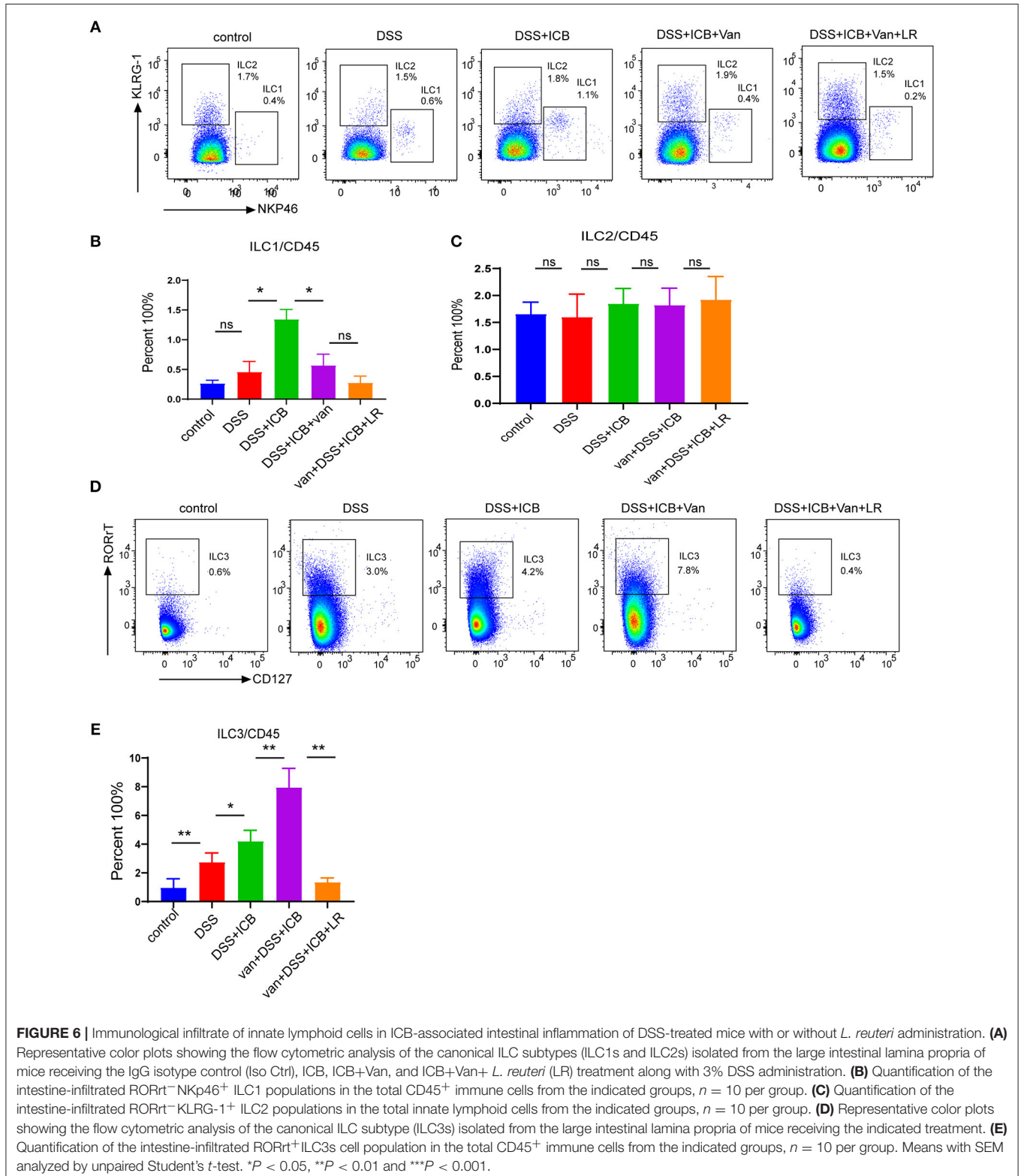
treatment also decreased the serum levels of the inflammatory cytokines KC, TNF- α , IFN- γ , and IL-6 in the DSS colitis mice (Figure 4F and Supplementary Figure S7). Taken together, our results demonstrate that coadministration of the probiotic *L. reuteri* could rescue the mice from the immunopathology induced by ICB-associated colitis.

L. reuteri Does Not Affect Antitumor Immunity of ICB

We further examined whether the amelioration of the immunopathology by *L. reuteri* occurs at the cost of ICB efficacy. Treatment with the probiotic *L. reuteri* did not affect the growth kinetics of established B16 melanoma tumors with ICB administration (Figure 5A). Tumors of comparable size were found in *L. reuteri*-treated mice and in PBS-treated control mice administered with ICB treatment on day 19 post-inoculation (Figure 5B). Probiotic *L. reuteri* treatment also did not affect the total survival of mice bearing established B16 melanoma tumors (Figure 5C). Flow data also showed that *L. reuteri* administration

was accomplished without significant changes in the tumor-infiltrating T cells, predicting a minor or no effect on the antitumor effect of the immunotherapy (Figure 5D). Moreover,

a single *L. reuteri* administration has no effect on the growth kinetics of established B16 melanoma tumors (Figure 5E). These data suggest that *L. reuteri* ameliorated the immunopathology



without compromising the therapeutic efficacy of ICB against melanoma in this system.

The Immune Regulatory Function of *L. reuteri* Is Associated With Intestinal ILC3 Cells

We next investigated the immunologic mechanism underlying the observed amelioration of colitis in *L. reuteri*-treated mice. To evaluate the effect of *L. reuteri* on the immune system in this DSS colitis model, we analyzed the profile of the immune cells in the gut, and we found that administration of ICB increases the frequency of CD8⁺ T cells. However, we did not observe any significant differences between PBS- and *L. reuteri*-treated mice with respect to the amounts of CD45⁺ immune cells, myeloid cells or T cells isolated from the colons (**Supplementary Figures S8A–D**).

Recently, a newly identified class of innate lymphoid cells, termed ILCs, has been shown to play a pivotal role in the development of IBD and shaped by microbiome (27–30). To evaluate whether ILCs were involved in the immunological mechanism underlying the observed amelioration of the colitis in *L. reuteri*-treated mice, we first characterized the three canonical subsets of helper-like ILCs. To this end, we used combined biomarkers to analyze the RORgt-NKp46⁺ ILC1s, RORgt-KLRG-1⁺ ILC2s, and RORgt+ILC3s by flow cytometry (31) (**Supplementary Figure S9**). The flow cytometric analysis revealed that although there were no significant changes in the total numbers of CD3⁺ T cells in any of the groups, we did find dramatic differences in the composition of the innate lymphoid cells among the different treatment groups. Interestingly, the magnitudes of the changes in ILC abundance were highly distinct between the subgroups, and the relative changes in the ILC1 and ILC2 subsets within each subgroup were not significant (**Figures 6A–C**). Of note, the spectrum of the changes in the abundance of the group 3 innate lymphoid cells (ILC3s) corresponded exactly with the severity of the immunopathology associated with DSS colitis (**Figure 6D**). Group 3 innate lymphoid cells (ILC3s) are an emerging class of innate lymphocytes that play a critical role in regulating mucosal homeostasis. In our DSS colitis model, the severity of that ICB-associated colitis was associated with increased mucosal numbers of ILC3s, but not with changes in the numbers of ILC1s and ILC2s, suggesting that ILC3s are involved in the immunopathology of ICB-associated colitis. *L. reuteri* administration dramatically decreases the mucosal numbers of ILC3s ($P < 0.01$) (**Figure 6E**) and level of function cytokines IL23 and IL17 (**Supplementary Figures S10A–C**), which therapeutically prevented colitis in ICB-treated mice (**Figure 6D**). Thus, it is likely that *L. reuteri* acts on the immunopathology of ICB-associated colitis primarily by affecting the local number of ILC3s.

DISCUSSION

Despite achieving great clinical success, ICB immunotherapy as a monotherapy or as a part of various combinational

strategies has challenges and limitations including the development of irAEs. ICB-associated colitis, one of the irAEs, is quite frequent and severe and is routinely treated with immunosuppressive therapy, which has significant side effects that diminished the antitumor response. Our study demonstrates a role for *Lactobacillus* in eliminating the intestinal immunopathology associated with ICB associated colitis.

Immune checkpoint inhibition is a recently introduced, innovative form of cancer immunotherapy that aims to eliminate inhibitory costimulatory signals from T cells, mainly tumor-specific cytotoxic CD8⁺ T cells, via blockade of cytotoxic T-lymphocyte associated protein-4 (CTLA-4), and/or programmed death protein-1 (PD-1)/PD-ligand 1 (PD-L1) (32–34). The treatment consists of administration of monoclonal antibodies that target CTLA-4 (ipilimumab, tremelimumab), PD-1 (pembrolizumab, nivolumab), and PD-L1 (atezolizumab, avelumab, durvalumab) to restore the cytotoxic function of lymphocytes and to induce effective antineoplastic responses (35). In contrast, elimination of immunoregulatory control by T cell-dependent inhibitory pathways may lead to unrestrained activation of effector immune responses that ultimately result in irAEs, which can involve several organs and lead to serious damage. Gastrointestinal toxicity is among the most common and potentially serious irAE and the most frequent reason for discontinuing immunotherapy. Overt colonic inflammation after anti-CTLA-4 and/or anti-PD-1/PDL-1 immunotherapy is referred to as ICB associated colitis (36).

ICB-associated colitis acts as a distinct form of colitis that is characterized by flares reminiscent of those associated with IBD. Elucidation of the mechanisms involved in its immunopathogenesis will greatly enhance our understanding and therapeutic management of immune-mediated colitis (8). In our DSS model, we demonstrated that ICB treatment can aggregate the immunopathology of colitis. Our results with the B16 tumor model and DSS colitis are consistent with the clinical observations in patients who received ipilimumab (anti-CTLA-4 antibody), and/or nivolumab (anti-PD-1 antibody). The gut microbiota can drive the maturation and function of the immune system. Indeed, the bacterial microbiota profiling performed using 16S ribosomal RNA sequencing on the Illumina MiSeq platform revealed that the gut microbiota community structure, in particular, the microbial species present and their relative amounts, are associated with immunopathology of ICB-associated colitis. In our ICB-associated colitis model, the relative abundance of *Lactobacillus* was significantly lower in the stool of ICB-treated mice compared to the relative populations in the control and DSS administration only groups. Consistent with our finding, specific probiotic strains of *L. reuteri* were recently shown to suppress intestinal inflammation in a trinitrobenzene sulfonic acid (TNBS)-induced mouse colitis model (37). Taken together, these results suggest that some specific intestinal bacteria species may orchestrate the initiation of inflammation whereas other subsets may have a role in perpetuating ICB associated colitis.

In an effort to provide mechanistic evidence for the microbiota-ICB colitis connection, Wang et al. (19) recently administered a neutralizing anti-CTLA antibody to DSS-treated mice, and they found that compared with mice receiving the isotype-treatment, anti-CTLA-4 blockade led to more severe colitis that was further aggravated following pretreatment with the antibiotic vancomycin, suggesting a mitigating effect of the Gram-positive components of the microflora. In our study, we confirmed that administration of the probiotic *L. reuteri* could rescue the mice from the immunopathology of DSS-induced colitis. This rescue was accomplished without significant changes in the systemic or local numbers of T cells, predicting a minor or no effect on the antitumor effect of the immunotherapy. ILC3s are involved in the immunopathology of ICB-associated colitis. *L. reuteri* administration dramatically decreases the mucosal numbers of ILC3s. Interestingly, it is shown that tryptophan catabolites of *L. reuteri* have been recognized as ligands for aryl hydrocarbon receptor (AhR) (38). The introduction of *L. reuteri* was also shown to promote antitumor responses after PD-L1 blockade by augmenting dendritic cell function. Moreover, *L. reuteri* administration fully ameliorated the immunopathology of ICB-associated colitis without compromising the therapeutic efficacy of combined ICB against melanoma in our system.

Currently, many studies indicate a role for innate lymphoid cells (ILCs) in the pathogenesis of IBD (29, 39). Innate lymphoid cells (ILCs) are a recently discovered group of innate immune cells. ILCs are detected in many organs and are especially enriched in the mucosal tissues of the human body. Some evidence has been provided to show that ILCs play crucial roles in the control of tissue homeostasis, act as effector cells in the immune responses to infections and function in inflammatory conditions (40). Indeed, several studies have reported that the ILC composition and function changes in the lamina propria of IBD patients (27, 41–44). In the majority of human studies, a potential role for ILCs was also found to be involved in Crohn's disease progression (29). The ILC component consists of three distinct groups: group 1 ILCs (ILC1s), group 2 ILCs (ILC2s), and group 3 ILCs (ILC3s). ILC3s have been shown to produce robust amounts of IL-22 and have important roles in maintaining the integrity of the intestinal barrier and promoting mucosal healing in IBD patients (45). In our DSS colitis model, the severity of the ICB-associated colitis was associated with increased mucosal numbers of group 3 innate lymphoid cells (ILC3s) and not with the levels of ILC1s and ILC2s, suggesting that ILC3s are the major innate lymphoid cell type involved in the immunopathology of ICB-associated colitis. *L. reuteri* administration dramatically decreased the mucosal numbers of ILC3s and therapeutically prevented colitis in the ICB-treated mice. Thus, it is likely that *L. reuteri* affects the immunopathology of ICB-associated colitis primarily by altering the local number of ILC3s. It should be noted that more research in this area is needed to clarify and integrate the current knowledge to improve treatment strategies for patients with ICB-associated colitis.

In summary, in this study, we provide strong evidence that modulation of the gut microbiome may abrogate ICB-associated colitis. If the same mechanisms are present in humans, this approach may provide a means to reduce or ameliorate the autoimmunity condition that often accompanies checkpoint blockade therapies, without diminishing the anticancer responses. This principle could apply to other checkpoint-related immunotherapies, such as the use of Tim3/LAG3-targeting antibodies or immunotherapy approaches directed against CAR-T cells and adoptive transfer.

DATA AVAILABILITY

The 16S rRNA sequence data have been deposited in the NCBI BioProject with accession number PRJNA525923.

ETHICS STATEMENT

The study protocol was reviewed and approved by the Institutional Review Board and Ethics Committee of Xinhua Hospital, Shanghai Jiao Tong University School of Medicine, China. All animal procedures were performed according to national guidelines and approved by the Animal Ethical and Experimental Committee of Xinhua Hospital, Shanghai Jiao Tong University School of Medicine.

AUTHOR CONTRIBUTIONS

LS and XY supervised the whole project, designed the experiments, analyzed data, and wrote the manuscript. TW performed the most experiments, analyzed data, and prepared the figures. NZ, QL, LJ, and BH contributed to some experiments and provided technical support. All authors read and approved the final manuscript.

FUNDING

This work was partly supported by National Natural Science Foundation of China (No. 81772525, 81672363, 81472244, 81402148).

ACKNOWLEDGMENTS

We thank our colleagues in the Department of clinical laboratory for helpful discussions and valuable assistance.

SUPPLEMENTARY MATERIAL

The Supplementary Material for this article can be found online at: <https://www.frontiersin.org/articles/10.3389/fimmu.2019.01235/full#supplementary-material>

REFERENCES

- Khalil DN, Smith EL, Brentjens RJ, Wolchok JD. The future of cancer treatment: immunomodulation, CARs and combination immunotherapy. *Nat Rev Clin Oncol.* (2016) 13:273–90. doi: 10.1038/nrclinonc.2016.25
- Postow MA, Chesney J, Pavlick AC, Robert C, Grossmann K, McDermott D, et al. Nivolumab and ipilimumab versus ipilimumab in untreated melanoma. *N Engl J Med.* (2015) 372:2006–17. doi: 10.1056/NEJMoa1414428
- Postow MA, Sidlow R, Hellmann MD. Immune-related adverse events associated with immune checkpoint blockade. *N Engl J Med.* (2018) 378:158–68. doi: 10.1056/NEJMra1703481
- Hodi FS, O'Day SJ, McDermott DE, Weber RW, Sosman JA, Haanen JB, et al. Improved survival with ipilimumab in patients with metastatic melanoma. *N Engl J Med.* (2010) 363:711–23. doi: 10.1056/NEJMoa1003466
- Brahmer JR, Tykodi SS, Chow LQ, Hwu WJ, Topalian SL, Hwu P, et al. Safety and activity of anti-PD-L1 antibody in patients with advanced cancer. *N Engl J Med.* (2012) 366:2455–65. doi: 10.1056/NEJMoa1200694
- Topalian SL, Hodi FS, Brahmer JR, Gettinger SN, Smith DC, McDermott DE, et al. Safety, activity, and immune correlates of anti-PD-1 antibody in cancer. *N Engl J Med.* (2012) 366:2443–54. doi: 10.1056/NEJMoa1200690
- Michot JM, Bigenwald C, Champiat S, Collin M, Carbonnel F, Postel-Vinay S, et al. Immune-related adverse events with immune checkpoint blockade: a comprehensive review. *Eur J Cancer.* (2016) 54:139–48. doi: 10.1016/j.ejca.2015.11.016
- Siakavellas SI, Bamias G. Checkpoint inhibitor colitis: a new model of inflammatory bowel disease? *Curr Opin Gastroenterol.* (2018) 34:377–83. doi: 10.1097/MOG.0000000000000482
- Chen JH, Pezhohou MK, Lauwers GY, Masia R. Histopathologic features of colitis due to immunotherapy with anti-PD-1 antibodies. *Am J Surg Pathol.* (2017) 41:643–54. doi: 10.1097/PAS.0000000000000829
- Dadu R, Zobniw C, Diab A. Managing adverse events with immune checkpoint agents. *Cancer J.* (2016) 22:121–9. doi: 10.1097/PPO.0000000000000186
- Wang Y, Wiesnoski DH, Helmink BA, Gopalakrishnan V, Choi K, DuPont HL, et al. Fecal microbiota transplantation for refractory immune checkpoint inhibitor-associated colitis. *Nat Med.* (2018) 24:1804–8. doi: 10.1038/s41591-018-0238-9
- Tarhini AA, Zahoor H, Lin Y, Malhotra U, Sander C, Butterfield LH, et al. Baseline circulating IL-17 predicts toxicity while TGF-beta1 and IL-10 are prognostic of relapse in ipilimumab neoadjuvant therapy of melanoma. *J Immunother Cancer.* (2015) 3:39. doi: 10.1186/s40425-015-0081-1
- Matson V, Fessler J, Bao R, Chongsawat T, Zha Y, Alegre ML, et al. The commensal microbiome is associated with anti-PD-1 efficacy in metastatic melanoma patients. *Science.* (2018) 359:104–8. doi: 10.1126/science.aao3290
- Gopalakrishnan V, Spencer CN, Nezi L, Reuben A, Andrews MC, Karpinetz TV, et al. Gut microbiome modulates response to anti-PD-1 immunotherapy in melanoma patients. *Science.* (2018) 359:97–103. doi: 10.1126/science.aan4236
- Routy B, Le Chatelier E, Derosa L, Duong CPM, Alou MT, Daillere R, et al. Gut microbiome influences efficacy of PD-1-based immunotherapy against epithelial tumors. *Science.* (2018) 359:91–7.
- Vetizou M, Pitt JM, Daillere R, Lepage P, Waldschmitt N, Flament C, et al. Anticancer immunotherapy by CTLA-4 blockade relies on the gut microbiota. *Science.* (2015) 350:1079–84. doi: 10.1126/science.aad1329
- Sivan A, Corrales L, Hubert N, Williams JB, Aquino-Michaels K, Earley ZM, et al. Commensal Bifidobacterium promotes antitumor immunity and facilitates anti-PD-L1 efficacy. *Science.* (2015) 350:1084–9. doi: 10.1126/science.aac4255
- Dubin K, Callahan MK, Ren B, Khanin R, Viale A, Ling L, et al. Intestinal microbiome analyses identify melanoma patients at risk for checkpoint-blockade-induced colitis. *Nat Commun.* (2016) 7:10391. doi: 10.1038/ncomms10391
- Wang F, Yin Q, Chen L, Davis MM. Bifidobacterium can mitigate intestinal immunopathology in the context of CTLA-4 blockade. *Proc Natl Acad Sci USA.* (2018) 115:157–61. doi: 10.1073/pnas.1712901115
- Bertin Y, Habouzit C, Duniere L, Laurier M, Durand A, Duchez D, et al. *Lactobacillus reuteri* suppresses *E. coli* O157:H7 in bovine ruminal fluid: toward a pre-slaughter strategy to improve food safety? *PLoS ONE.* (2017) 12:e0187229. doi: 10.1371/journal.pone.0187229
- He B, Hoang TK, Wang T, Ferris M, Taylor CM, Tian X, et al. Resetting microbiota by *Lactobacillus reuteri* inhibits T reg deficiency-induced autoimmunity via adenosine A2A receptors. *J Exp Med.* (2017) 214:107–23. doi: 10.1084/jem.20160961
- Sun MC, Zhang FC, Yin X, Cheng BJ, Zhao CH, Wang YL, et al. *Lactobacillus reuteri* F-9-35 prevents DSS-induced colitis by inhibiting proinflammatory gene expression and restoring the gut microbiota in mice. *J Food Sci.* (2018) 83:2645–52. doi: 10.1111/1750-3841.14326
- Schreiber O, Petersson J, Phillipson M, Perry M, Roos S, Holm L. *Lactobacillus reuteri* prevents colitis by reducing P-selectin-associated leukocyte- and platelet-endothelial cell interactions. *Am J Physiol Gastrointest Liver Physiol.* (2009) 296:G534–42. doi: 10.1152/ajpgi.90470.2008
- Huang G, Sun K, Yin S, Jiang B, Chen Y, Gong Y, et al. Burn injury leads to increase in relative abundance of opportunistic pathogens in the rat gastrointestinal microbiome. *Front Microbiol.* (2017) 8:1237. doi: 10.3389/fmicb.2017.01237
- Lee SH, Lee Y, Park JS, Cho YJ, Yoon HI, Lee CT, et al. Characterization of microbiota in bronchiectasis patients with different disease severities. *J Clin Med.* (2018) 7:E429. doi: 10.3390/jcm7110429
- Franzosa EA, Sirota-Madi A, Avila-Pacheco J, Fornelos N, Haiser HJ, Reinker S, et al. Gut microbiome structure and metabolic activity in inflammatory bowel disease. *Nat Microbiol.* (2019) 4:293–305. doi: 10.1038/s41564-018-0306-4
- Buela KA, Omenetti S, Pizarro TT. Cross-talk between type 3 innate lymphoid cells and the gut microbiota in inflammatory bowel disease. *Curr Opin Gastroenterol.* (2015) 31:449–55. doi: 10.1097/MOG.0000000000000217
- Gury-BenAri M, Thaiss CA, Serafini N, Winter DR, Giladi A, Lara-Astiaso D, et al. The Spectrum and regulatory landscape of intestinal innate lymphoid cells are shaped by the microbiome. *Cell.* (2016) 166:1231–46 e13. doi: 10.1016/j.cell.2016.07.043
- Forkel M, Mjosberg J. Dysregulation of group 3 innate lymphoid cells in the pathogenesis of inflammatory bowel disease. *Curr Allergy Asthma Rep.* (2016) 16:73. doi: 10.1007/s11882-016-0652-3
- Brasseit J, Kwong Chung CKC, Noti M, Zysset D, Hoheisel-Dickgreber N, Genitsch V, et al. Divergent roles of interferon-gamma and innate lymphoid cells in innate and adaptive immune cell-mediated intestinal inflammation. *Front Immunol.* (2018) 9:23. doi: 10.3389/fimmu.2018.00023
- Gronke K, Kofoed-Nielsen M, Diefenbach A. Isolation and flow cytometry analysis of innate lymphoid cells from the intestinal lamina propria. In: Clausen BE, Laman JD, editors. *Inflammation: Methods and Protocols.* New York, NY: Springer (2017). p. 255–65.
- Li X, Shao C, Shi Y, Han W. Lessons learned from the blockade of immune checkpoints in cancer immunotherapy. *J Hematol Oncol.* (2018) 11:31. doi: 10.1186/s13045-018-0578-4
- Li Y, Li F, Jiang F, Lv X, Zhang R, Lu A, et al. A mini-review for cancer immunotherapy: molecular understanding of PD-1/PD-L1 pathway & translational blockade of immune checkpoints. *Int J Mol Sci.* (2016) 17:E1151. doi: 10.3390/ijms17071151
- Pardoll DM. The blockade of immune checkpoints in cancer immunotherapy. *Nat Rev Cancer.* (2012) 12:252–64. doi: 10.1038/nrc3239
- Lee A, Sun S, Sandler A, Hoang T. Recent progress in therapeutic antibodies for cancer immunotherapy. *Curr Opin Chem Biol.* (2018) 44:56–65. doi: 10.1016/j.cbpa.2018.05.006
- Marin-Acevedo JA, Harris DM, Burton MC. Immunotherapy-induced colitis: an emerging problem for the hospitalist. *J Hosp Med.* (2018) 13:413–8. doi: 10.12788/jhm.2925
- Mu Q, Tavella VJ, Luo XM. Role of *Lactobacillus reuteri* in human health and diseases. *Front Microbiol.* (2018) 9:757. doi: 10.3389/fmicb.2018.00757
- Zelante T, Iannitti RG, Cunha C, De Luca A, Giovannini G, Pieraccini G, et al. Tryptophan catabolites from microbiota engage aryl hydrocarbon

- receptor and balance mucosal reactivity via interleukin-22. *Immunity*. (2013) 39:372–85. doi: 10.1016/j.immuni.2013.08.003
39. Castellanos JG, Woo V, Viladomiu M, Putzel G, Lima S, Diehl GE, et al. Microbiota-induced TNF-like ligand 1A Drives group 3 innate lymphoid cell-mediated barrier protection and intestinal T cell activation during colitis. *Immunity*. (2018) 49:1077–89.e5. doi: 10.1016/j.immuni.2018.10.014
40. Artis D, Spits H. The biology of innate lymphoid cells. *Nature*. (2015) 517:293–301. doi: 10.1038/nature14189
41. Wang S, Xia P, Chen Y, Qu Y, Xiong Z, Ye B, et al. Regulatory innate lymphoid cells control innate intestinal inflammation. *Cell*. (2017) 171:201–16 e18. doi: 10.1016/j.cell.2017.07.027
42. Withers DR, Hepworth MR, Wang X, Mackley EC, Halford EE, Dutton EE, et al. Transient inhibition of ROR-gammat therapeutically limits intestinal inflammation by reducing TH17 cells and preserving group 3 innate lymphoid cells. *Nat Med*. (2016) 22:319–23. doi: 10.1038/nm.4046
43. Fung TC, Bessman NJ, Hepworth MR, Kumar N, Shibata N, Kobuley D, et al. Lymphoid-tissue-resident commensal bacteria promote members of the IL-10 cytokine family to establish mutualism. *Immunity*. (2016) 44:634–46. doi: 10.1016/j.immuni.2016.02.019
44. Hepworth MR, Fung TC, Masur SH, Kelsen JR, McConnell FM, Dubrot J, et al. Group 3 innate lymphoid cells mediate intestinal selection of commensal bacteria-specific CD4(+) T cells. *Science*. (2015) 348:1031–5. doi: 10.1126/science.aaa4812
45. Longman RS, Diehl GE, Victorio DA, Huh JR, Galan C, Miraldi ER, et al. CX(3)CR1(+) mononuclear phagocytes support colitis-associated innate lymphoid cell production of IL-22. *J Exp Med*. (2014) 211:1571–83. doi: 10.1084/jem.20140678

Conflict of Interest Statement: The authors declare that the research was conducted in the absence of any commercial or financial relationships that could be construed as a potential conflict of interest.

Copyright © 2019 Wang, Zheng, Luo, Jiang, He, Yuan and Shen. This is an open-access article distributed under the terms of the Creative Commons Attribution License (CC BY). The use, distribution or reproduction in other forums is permitted, provided the original author(s) and the copyright owner(s) are credited and that the original publication in this journal is cited, in accordance with accepted academic practice. No use, distribution or reproduction is permitted which does not comply with these terms.